International Journal of Coal Geology 279 (2023) 104376

Contents lists available at ScienceDirect

International Journal of Coal Geology

journal homepage: www.elsevier.com/locate/coal

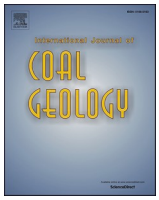

Experimental investigation of CO2-CH4 core flooding in large intact bituminous coal cores using bespoke hydrostatic core holder

Maram Almolliyeh [a], Sivachidambaram Sadasivam [a,*], Min Chen [a], Shakil Masum [a], Hywel Rhys Thomas [a]

[a] Geoenvironmental Research Centre (GRC), School of Engineering, Cardiff University, The Queen's Buildings, The Parade, Cardiff CF24 3AA, United Kingdom

ARTICLE INFO

Keywords:
Coal core
CO2-CH4 Core flooding
Permeability
CO2 storage
CO2-ECBM

ABSTRACT

This paper presents the CO2-CH4 core flooding and permeability studies conducted with large intact coal core samples. A bespoke core holder was designed and commissioned to conduct the core flooding experiments. The CO2 and CH4 core flooding experiments were performed to understand the CH4 displacement efficiency of CO2 from the coal cores and the permeabilities of CO2 and CH4 during the core flooding. The CO2-CH4 gas displacement experiments were performed on intact coal cores of 9.9 cm in diameter with varying lengths to make up 60 cm-long cores that were extracted from coal blocks using a diamond core-drilling machine. The CO2 and CH4 core flooding experiments were conducted using the core holder at maximum of 1450 psi confining pressures and at 298.15 K. A constant gas flow rate of 1 mL/min was maintained to flood the core with an outlet backpressure set at 25 to 30 ± 2 psi. The core holder is equipped with two differential pressure taps to measure the pressure change along the core length to measure the differing permeability along the core lengths which is difficult to observe in the smaller size intact samples. Both coals, EMB and ZM, showed favourable CH4 displacement efficiencies of CO2 about 96.5% and 99.7%, respectively. The dependency of the core lengths on the permeability measurements is more pronounced in the results obtained in the current study. The results indicated a decreasing trend in CO2 permeability and increasing CH4 permeability during CO2 injection. The observation indicated CO2 adsorption and CH4 displacement. Overall, the core flooding experiments improved the current understanding of CO2-CH4 core flooding by showing the core size dependence in permeability measurement experiments. In contrast to the single species CO2 flow experiments, the permeability variation during the CO2-CH4 flooding and the CH4 sweeping efficiency of CO2 provided insights into the CO2-ECBM operational design.

1. Introduction

Accurate estimation and sound understanding of coal permeability and its behaviour are crucial for successful coal-seam CO2 storage and recovery of coalbed gases. Large amount of research studies has investigated coal-seam permeability behaviours over the past decades (De Silva and Ranjith, 2013; Gensterblum et al., 2014; Harpalani and Chen, 1997; Li et al., 2014; Liu et al., 2011; Mazumder et al., 2012; Meng et al., 2021; Mukherjee et al., 2021; Pan et al., 2010; Viete and Ranjith, 2006; Wang et al., 2011). However, there is a significant limitation inherent to the existing studies and it is associated with the coal sample sizes. They are mainly based on powdered, crushed, or small intact cores (in tens of millimetre scale) samples which fails to preserve macro-scale features and/ structural composition of large intact coal cores or samples. This can eventually lead to estimation of permeability values that are significantly deviated from the field or in-situ values.

Due to the molecular sieving effect, CO2 permeability was often found lower than He permeability for porous rocks (Cui et al., 2009). CO2 sorption causes swelling and shrinkage of coal structure (Hol et al., 2012). Along with coal swelling/shrinkage due to CO_2 gas adsorption/ desorption, confining pressure and pore pressure significantly influence coal-seam gas permeability behaviour (Seidle et al., 1992; Siriwardane et al., 2009; Vishal et al., 2013).

Understanding the permeability of CO2 and CH4 displacement efficiency in coal seams under field conditions is important for controlling the injection process. Experiments were conducted in the context of CO2 enhanced coal bed methane recovery (CO2-ECBM) to better understand CO2 permeability with displacement of CH4. High-pressure supercritical

* Corresponding author.
E-mail address: sadasivams@cardiff.ac.uk (S. Sadasivam).

https://doi.org/10.1016/j.coal.2023.104376
Received 10 April 2023; Received in revised form 2 October 2023; Accepted 7 October 2023
Available online 10 October 2023

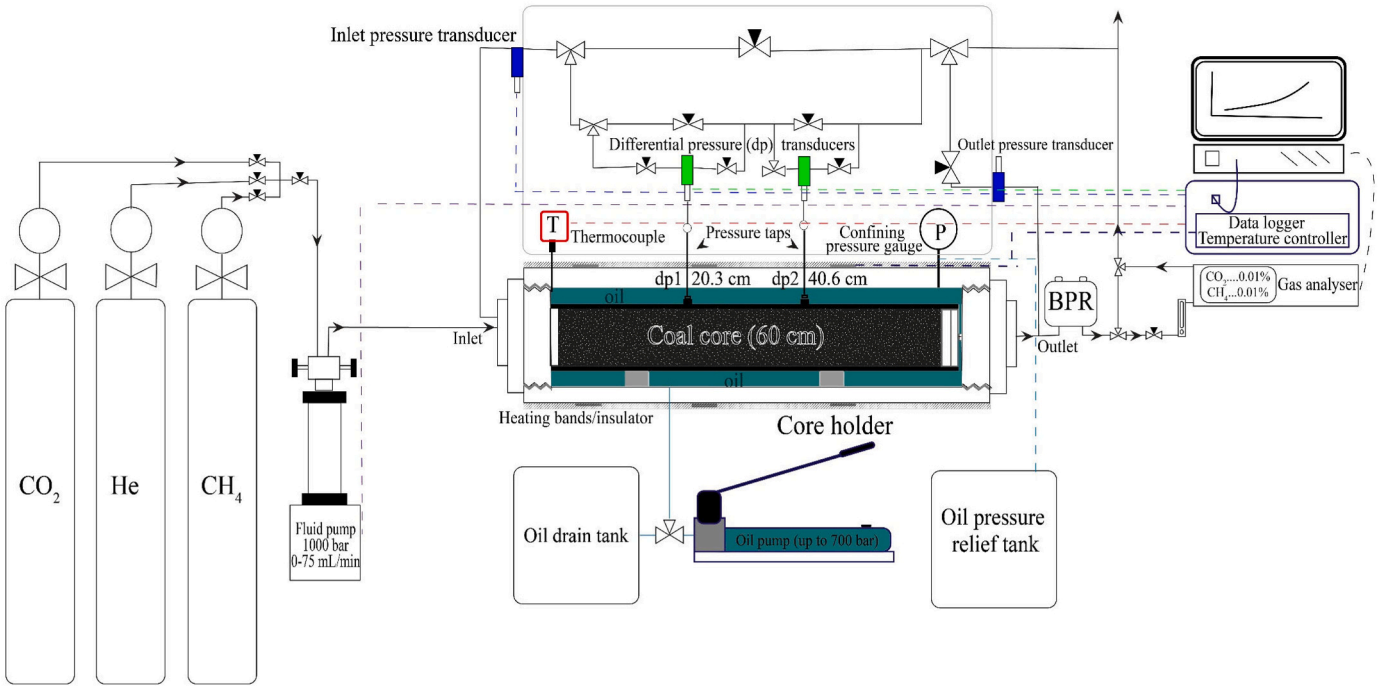

Fig. 1. Schematic of the bespoke hydrostatic core holder.

injection has been considered so far to achieve high density. However, the confining stress limits injectivity, and shallow level CO2 injection has been considered (Chen et al., 2018). Most experiments were conducted with a few centimetres of lengths/diameters of samples, and the large samples were made up of pulverised samples. In most of the experiments, the permeability has been calculated using the inlet and outlet pressure values from the core holder experimental setup, which may not represent the variable permeability within the coal samples (De Silva and Ranjith, 2013; Liu et al., 2022; Mazumder and Wolf, 2008; Niu et al., 2020; Ranathunga et al., 2017; Sander et al., 2014; Shi et al., 2008; Stephen et al., 2014; Zhang and Ranjith, 2019; Zhou et al., 2013).

It has been clearly understood that CO2 displaces CH4 from the coal seam and that the removal efficiency of CO2 is superior to that of CH4. The reported efficiency obtained for CO2 injection was good enough to remove 99% of the methane. However, displacing CO2 by CH4 was less efficient (71% and 95%), indicating the coal's preference for CO2 over CH4 (Sander et al., 2014). Core flooding experiments conducted with 12 MPa confining pressure (representing 500–600 m depth) showed that the CO2 injection improved the efficiency of CH4 recovery (over 90%) compared to the natural recovery method (51.7%). Meanwhile, the rapid breakthrough of CO2 complicates the gas separation process (Zhang and Ranjith, 2019), which pertains to the flooding tests under low injection pressures. Similar results were observed by Ranathunga et al. (2017), showed that the CO2 injection could completely drive the CH4 out. The displacement ratio, CO_2 breakthrough time, and CO_2 storage capacity are identified as important parameters affecting the carbon sequestration application (Hadi Mosleh et al., 2017).

Limited experiments explored the CO2-CH4-CO2 flooding under gas with back pressure set up. Flooding experiments with back pressure experiments showed that increasing injection pressures improved the gas permeability and adsorption by increasing the matrix swell; however, the increase in the confining pressures reduced the CO2 permeability. The CO2 permeability was found to be lower than the CH4 permeability due to the adsorption effect (Niu et al., 2020; Zhou et al., 2013). The CO2 core flooding also induces the development of fracture lines in large intact coal samples and increases the pore volumes, which have been identified in uniaxial compression tests (Hol et al., 2012; Larsen, 2004; Li et al., 2010; Liu et al., 2015; Zagorščak and Thomas, 2018).

From the gathered knowledge, the random permeability of CO2 and CH4 in the coal samples has not been clearly understood. The injection pressures affect the dispersion rates of gases during the core flooding, indicating molecular diffusion and convection, which further intrigues the idea that the CH4-CO2 mixed gas flow through the core samples (permeability) should be investigated during the displacement process (Shi et al., 2008; Yin et al., 2017). The triaxial method and Hassler type hydrostatic core holders are the most commonly used techniques to measure coal permeability. The Hassler type core holders are best equipped for developing confining pressure and measuring pressure drop along the core (De Silva and Ranjith, 2013) and have recently sparked interest among scientists and technical cohorts. Intact coal-core samples studied thus far, mostly, ranged from 10 to 60 mm. De Silva and Ranjith (2013) used a reconstructed sample made of pulverised coal (< 3 mm particle size) to make a coal core of c.a. 830 mm length and 200 mm diameter. As mentioned earlier, such samples fail to adequately preserve structural integrity or natural flow channels of a coal deposit. Therefore, larger intact natural samples that could be obtained from a target seam for coal-seam CO_2 storage should be investigated. Hence, this is the focus of this study, and it aims to advance the knowledge gaps of existing literatures, especially, associated with permeability behaviour of large intact coal core samples.

2. Experimental methodology

2.1. The pressure-tapped hydrostatic core holder

The hydrostatic core holder is a state-of-the-art permeability measurement equipment designed and commissioned for the specific purpose of conducting CH4/CO2 core flooding experiments. The major component of the experimental setup is supplied by the Core Laboratories LP, Tulsa, Oklahoma, and Sanchez, France. Fig. 1 shows the schematic of the experimental setup. The main components are described below.

(i) A fluid pump capable of injecting fluids up to 1000 bar pressure at flow rates between 0 and 75 mL/min.

Table 1
Properties of coal samples from Experimental Mine Barbara (EMB) and Ziemowit mine (ZM).

Properties	EMB	ZM
Moisture content in analytical sample (%)	7.47	6.77
Ash content (%)	7.64	5.47
Volatile matter content (%)	30.49	35.91
Gross calorific value (kJ/kg)	27,224	28,782
Net calorific value (kJ/kg)	26,103	27,581
Total sulphur content (%)	0.99	0.64
Total carbon content (%)	68.62	69.6
Total Hydrogen content (%)	4.3	4.64
Nitrogen content	4.3	0.91

Table 2
gas permeability test conditions.

Sample	Tests/	Conditions
EMB cores	• He Permeability -CO_2 Permeability • CO2-CH4-CO2 Exchange • Pressure model validations	Confining pressure: 7.5 MPa (1088 psi) and 10 MPa (1450 psi). Temperature: 298.15 K. Flow rate: 1.67×10^{-08} m^3/s. Backup pore pressure: 25 psi.
ZM cores	• He Permeability -CO_2 Permeability • CO2-CH4-CO2 Exchange	Confining pressure: 10 MPa (1450 psi). Temperature: 298.15 K. Flow rate: 1.67×10^{-08} m^3/s. Backup pore pressure: 25 to 30 psi.

(ii) A pressure-tapped core holder capable of operating at confining pressures up to 700 bars and gas injection pressures up to 256 bar.
(iii) The core holder can accommodate a maximum of 60 cm long and 10 cm diameter core samples. Two pressure taps, at 20.3 cm and 40.6 cm from the inlet face of the holder, was connected to two differential pressure transducers for measuring the pressure difference along the length of a core sample.
(iv) Two pressure transducers to measure the inlet and outlet gas pressures.
(v) A back pressure regulator (BPR) with pressure rating of 1000 bar. The backpressure was controlled by the dome pressure set using compressed air.
(vi) A hydraulic oil pump capable of developing 700 bar confining pressure and an oil pressure gauge with safety pressure relief valve.
(vii) A thermocouple and heating bands, connected to a temperature controller, to maintain temperatures up to 250 °C. The core holder is insulated with glass wool-aluminum insulator.
(viii) The core holder is connected to an X-Stream general purpose gas analyser manufactured by Emerson Ltd. to measure CO_2 and CH_4 compositions during a core flooding experiment.
(ix) The pump, the pressure transducers, and the temperature sensor are connected to a data logger.
(x) Experiments are controlled by the software supplied by CoreLab Ltd. and Sanchez Ltd.

2.2. Coal sample preparation

Large coal blocks were obtained from the Experimental Mine Barbara (referred to as EMB) coal "seam-310," located at 30 m depth, and the

Fig. 2. (a) Core drilling equipment, (b), (c) and (d) 9.9 cm diameter cores drilled out of large blocks, (e) EBM coal cores, (f) ZM coal cores, (g) cores wrapped in PTFE tapes, (h) Viton tube with pressure taps, (i) Viton tube with cores inserted and placed inside the core holder, (j) the gas tight plunger with gas outlet tube inserted to the Viton tube, and (k) the experiment ready hydrostatic core holder set up.

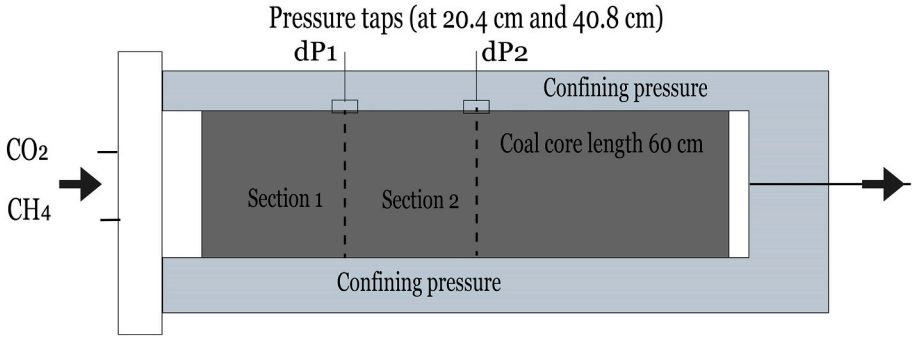

Fig. 3. Illustration of the pressure-taps and hypothetical segmentation of the core for calculating variable core permeability where 'Section 1' refers to the length of the core between the inlet and the pressure-tap dp1, and 'Section 2' refers to the length of the core from the inlet to the pressure-tap dp2.

Ziemowit mine (referred to as ZM), from a seam located at 900 m depth, Poland. The properties of both coal samples have been presented in Table 1. The core samples have been extracted from the large blocks. A 9.9-cm-diameter diamond bespoke core drill bit specially made for coal was pushed down in the large blocks in a slow and steady state to drill the cores (Fig. 2a, b, c, and d). The lateral movement of the drill bit was kept to a minimum and retracted at time intervals, and the longest cores extracted were used in the study. The core samples were obtained in various lengths, and the cross sections of the cores were polished with a diamond saw. Fig. 2e shows the core sample of EMB of lengths measuring 33 cm and 27 cm to make up the 60 cm long core. The connecting core faces were considered or mimicked the butt cleats of the coal seams. Fig. 2f shows the core sample of ZM of lengths measuring 6 cm, 13 cm, 12 cm, and 29 cm for the flooding experiments. The EMB coal sample is naturally more fractured than the ZM samples.

2.3. Core samples loading method

The coal cross sectional faces were polished to avoid 'vugs'. The cores were wrapped in a PTFE gas and liquid tight tapes (Fig. 2g). The 60 cm length core was then inserted into a Viton rubber sleeve with pressure tap ports (Fig. 2h). The sleeve with the coal sample was inserted to the inlet side cap of the core holder and placed inside the core holder (Fig. 2i). A plunger with a Viton O-ring and an outlet pipe was inserted at the outlet of the sleeve (Fig. 2j). Then the outlet end was closed with the core holder cap and the entire core holder was insulated with aluminum-glass wool material (Fig. 2k). The oil pump was used to fill the cavity around the sleeve with Enerpac hydraulic oil. To ensure oil leakage and a good seal minimum of 7.5 MPa confining pressure were required to be developed.

2.4. Methodology of coal core permeability measurement

The core flooding experiment was performed using CH_4, CO_2 and He gases. The experimental temperature was set at 298.15 K. Experiments were conducted at two confining pressures, 1088 psi (7.5 MPa) and 1450 psi (10.0 MPa) for EMB coal. Confining pressure was maintained at 1450 psi for ZM coal as the samples were from the depth of 900 m. Each core sample is initially injected with He followed by CO2 to obtain the single-species permeability using the gas pump. The pump was then filled with gases at a pressure of 70–80 psi. The pressure range is selected to maintain a low-pressure injection to simulate the horizontal well CO2 injections. After filling the pump with 300 mL of gas, the core was flooded at a flow rate of 1 mL/min. The gas outlet was monitored for the composition of the gas using the gas analyser. After measuring the single-species permeability the CO2 was replaced by CH4 injection. The core was flooded with CH4 until the CH4 concentration was close to 100% or the stable gas composition at the outlet. Once the core was flooded with CH4, the pump was refilled with CO2, and the CO2 was injected to replace the CH4. The experiment was run until the maximum percent of CH4 was replaced by CO2. These cycles of injections were used for determining the displacement efficiencies of CO2 and CH4 and permeability of each species during the displacement.

The outlet backpressure regulator (BPR) valve was set to 25 to 30 ± 2 psi so that the pressure builds up above these set values at the outlet could be released to the gas analyser to measure the percentage gas composition(s). The differential pressures (dP) along the core length were measured through the dP1 and dP2 pressure taps. The dP1 is the pressure differential between the inlet and 20.3 cm. dP2 is the pressure differential between dP1 and dP2 (at 40.6 cm). The core was theoretically sectioned Section 1 and Section 2 based on the locations of the

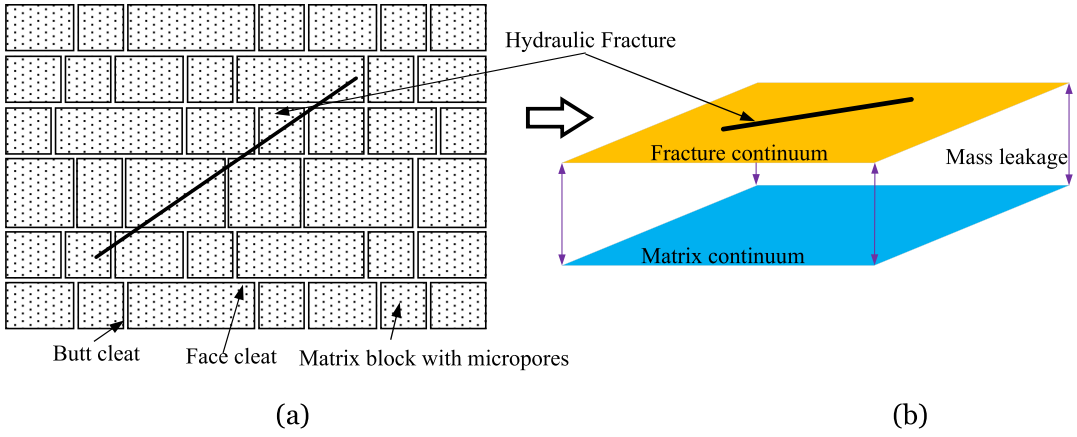

Fig. 4. (a) Schematic of naturally fractured coal: plan view and (b) the conceptualized dual porosity model embedded with hydraulic fracture. Experimental program and modelling are presented in Table 2.

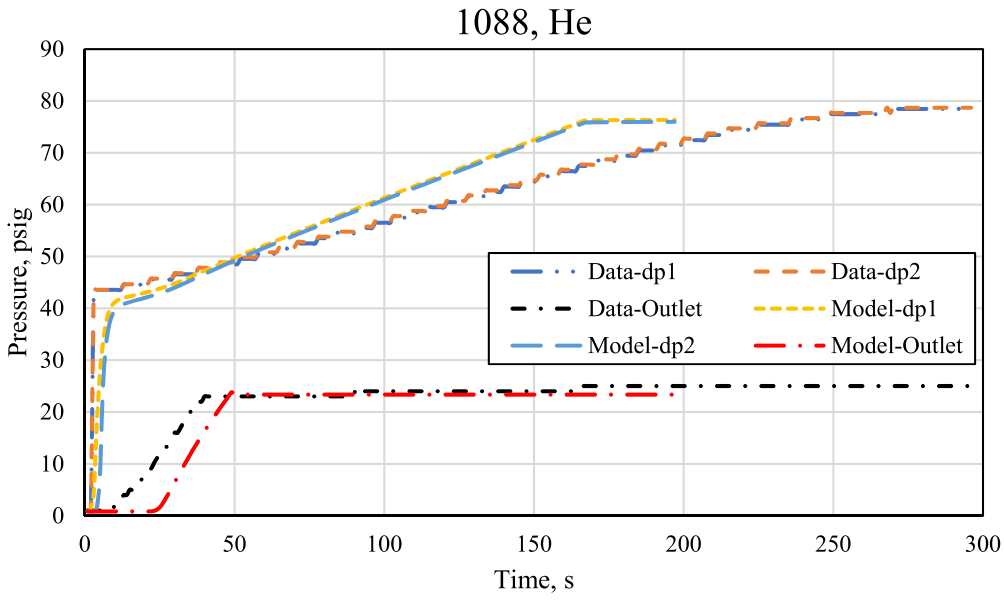

(a) 1088 psi confining pressure

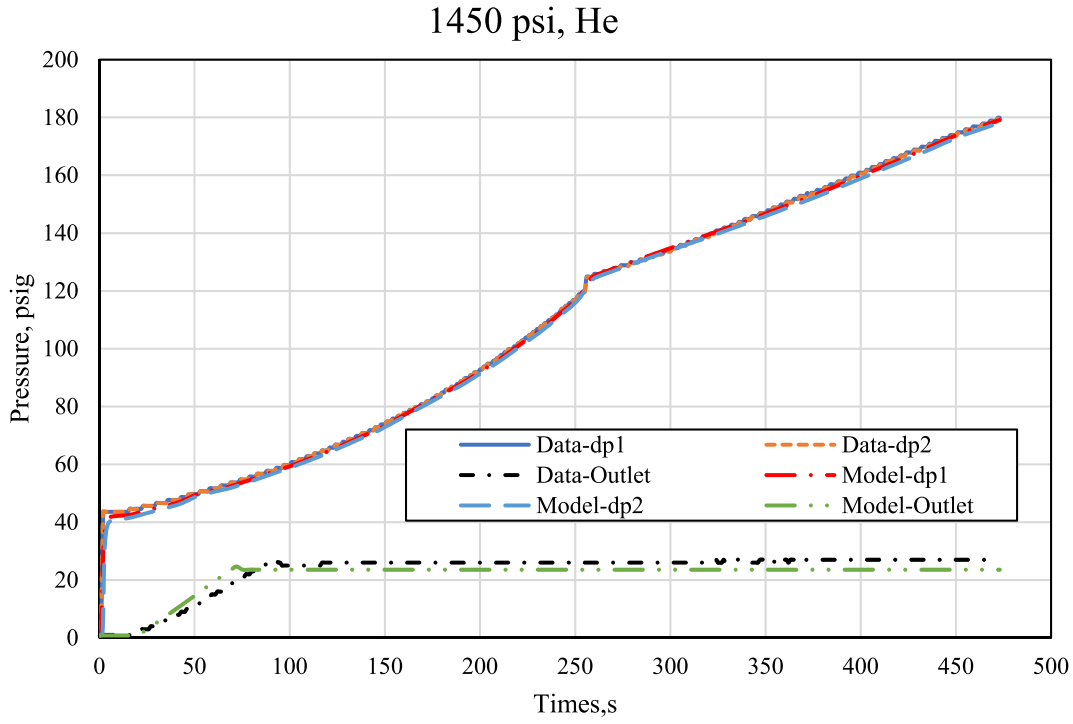

(b) 1450 psi confining pressure

Fig. 5. Comparison of gas pressure predicted by model with experimental data on He.

pressure taps to measure the random permeability within the core (Fig. 3).

The measured pressure values were used to calculate the apparent permeability of each species. For the mixed flow within the coal core, the partial pressures of CH4 and CO2 were calculated based on the gas composition measured at the outlet. The calculated partial pressure values at the inlet, dP1, dP2, and outlet were used to calculate the gas permeability following Darcy's law (API 40 Report., 1998; Liu et al., 2020).

$$k = \frac{2Q\,P_a \mu\, L}{A\left(P_i^2 - P_0^2\right)} \tag{1}$$

Where, k is permeability in m^2, Q is gas flow rate set at the pump (1.67×10^{-8} m^3/s), μ is viscosity in Pa.s, L is length of the core segments at dp1 (Section 1), dp2 (Section 2) or the overall length (20.3 cm, 40.6 cm and 60 cm), A is cross sectional area of the core (0.007854 m^2) and P_i, P_o and P_a represents inlet, outlet partial pressure of CH4 and CO2 and atmospheric (101,325 pa) pressures, respectively. The permeability calculated using the inlet pressure and outlet pressure is referred to as

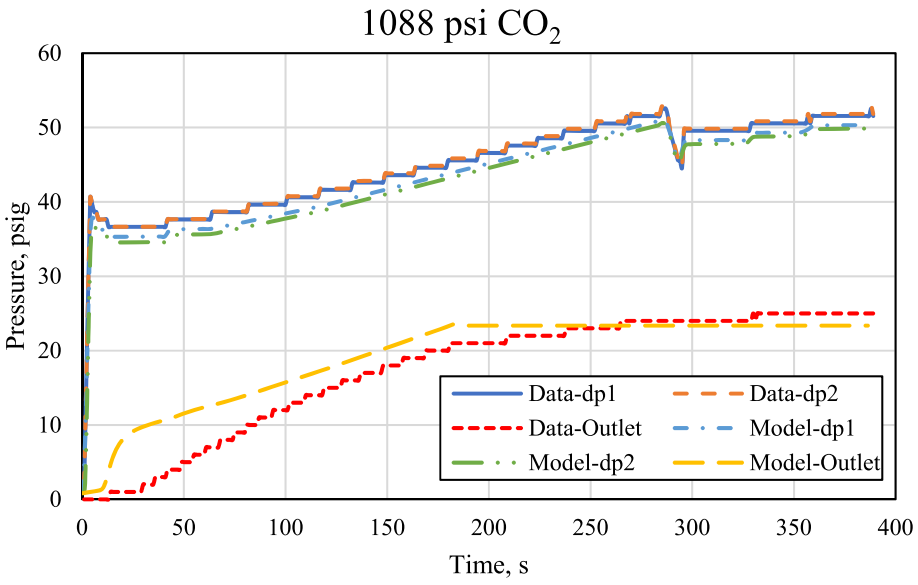

(a) 1088 psi confining pressure

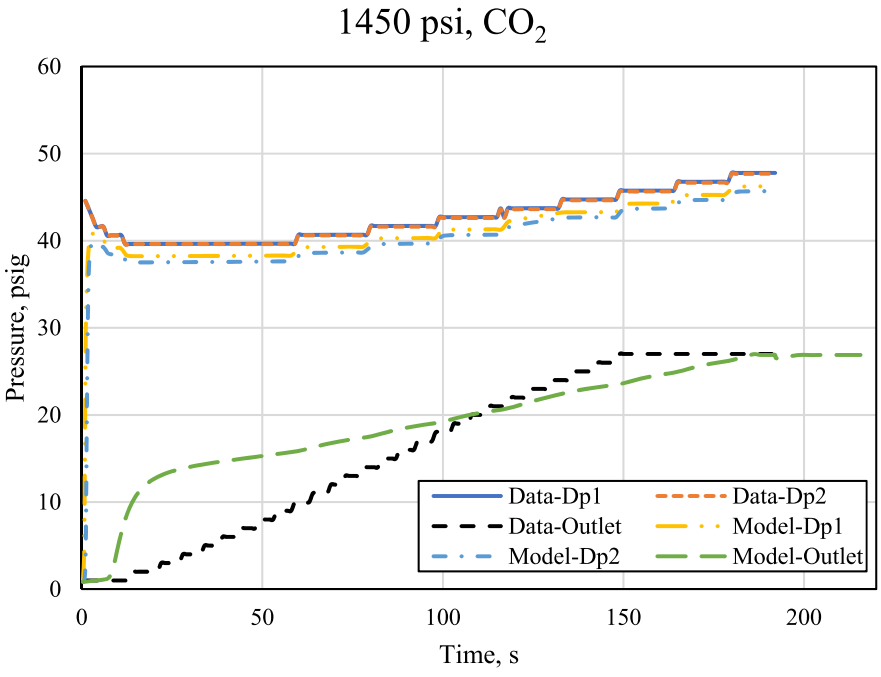

(b) 1450 psi confining pressure

Fig. 6. Comparison of gas pressure predicted by model with experimental data on CO_2.

the overall permeability, and the mean permeability values measured at Sections I, II, and overall length is referred to as the average permeability.

3. Numerical validation of gas pressures in of He and CO2 single species injection

Coalbeds are highly heterogeneous; they not only contain porous coal matrix but also have a well-defined and almost uniformly distributed cleat network, also called cleats, as shown in Fig. 4a. The coal matrix block is surrounded by intersecting face cleats and butt cleats. Therefore, coal reservoirs can be considered to comprise two different media: the matrix continuum (m), the fracture continuum (f), and the hydraulic fractures (F). Connected fractures provide a dominant pathway for fluid flow. In order to accurately describe flow behaviour and the related mechanical processes in fractured gas reservoirs, a dual porosity model is adopted, as shown in Fig. 4b. Both continua interact with one another through mass exchange. The theory of model development is presented in the supplementary section.

4. Results and discussions

4.1. Pressure measurements

4.1.1. Pressure measurements of He and CO_2 single species injection on EMB coal

Fig. 5a and b depict the inlet and outlet pressures over the course of the experiment for confining pressures of 1088 psi and 1450 psi, respectively. The back pressure valve was set at 25 ± 1 psi, and it took 45 min for the built-up pressure to reach the steady state condition (outlet 25 psi) for the confining pressure of 1088 psi, and approximately 90 min for the confining pressure of 1450 psi tests. After reaching the set-up pressure, the outlet pore pressure remained constant at (25 ± 2 psi) in both experiments. Helium is a non-adsorptive gas, and the continuous gas injection caused the inlet pressure to increase, with minimal gas pressure loss at the inlet due to permeation. The experiments showed that the inlet gas pressure varied from 40 psig to 80 psig under the 1088 psi confining pressure (Fig. 5a), and 40 psig to 180 psig for the 1450 psi confining pressure condition (Fig. 5b; psig refers to the gas pressure in psi). This behaviour suggests that the He permeability, with near zero acentric factor, is affected by injection pressure and the effective stress.

The CO_2 permeability test was conducted at similar boundary conditions to that of the He test (1088 psi and 1450 psi confining pressures, temperature of 298.15 K and backup pressure of 25 ± 2 Psi). However, the CO_2 inlet pressure was almost constant due to the CO_2 adsorption/desorption (Fig. 6). For 1088 psi, it took approximately 250 min to reach to the back pressure of 25 ± 2 psi. For higher confining pressure (1450 psi), it took 150 min reach the 25 ± 2 psi. At the inlet, CO2 pressure varied from 40 to 52 psi for 1088 psi confining pressure (Fig. 6a), and 44 psi to 48 psi for 1450 psi confining pressure (Fig. 6b).

At lower confining pressure, the CO2 permeates in a multidirectional path to the fractures by the coal swell and adsorbs with minimal influence of the confining stress, which reflects the longer permeation time to reach the set outlet pressure. At higher confining pressure, the flow is allowed only through the preferential paths, and the outlet reaches the set backup pressure faster. However, the influence of the confining pressure on the multidirectional gas movement is apparent through the permeability measurement.

The mean pore pressure ($p_m = \frac{(p_i+p_o)}{2}$) values observed was quite opposite to the He test, since CO_2 undergoes continuous adsorption-desorption. Therefore, the measured inlet pressure was almost steady against the fixed outlet pressure of 25 psi for CO2 (Fig. 6) and steep linear increase was observed for He after reaching set outlet pressure of 25 psi (Fig. 5).

Pressure differentials were measured along the core length at 20.3 cm (dP1) and 40.6 cm (dP2). The dP1 is the difference in pressures between the inlet and dp1. dP2 is the difference in pressures between dP1 and dP2.The differential pressures, dP1 and dP2, observed respectively at the pressure-taps dP1 and dP2 are converted to absolute pressures and presented in Figs. 5 and 6 for He and CO2 tests, respectively (Please refer the supplementary information for the raw data of the differential pressure measurements). The pressure differences quickly established for lower confining pressure as the gas permeate through the Section 1 faster than the section 2 (Fig. 6a). The gradual reduction in pressure at the entrance (Section 1, dP2) for the higher confining pressure shows that the permeation was much lower than the lower confining pressure (Fig. 6b). The dP2 values reflected the similar behaviour as the gas permeate quickly to the dP2, much higher pressure observed at 40.6 cm (dP2) than at 20.3 cm (dP2) under low confining pressure of 1088 psi reflected as negative differential pressure values (dP2 = pressure at 40.6 cm- pressure at 20.3 cm) (Fig. 6a). Under high confining pressure (1450 psi), the pressure at 40.6 cm (dP2) were much lower than at 20.3 cm (dP1) as the gas was not quickly permeating through between dP1 to dP2 reflected as positive differential pressure values at dP2 (Fig. 6b).

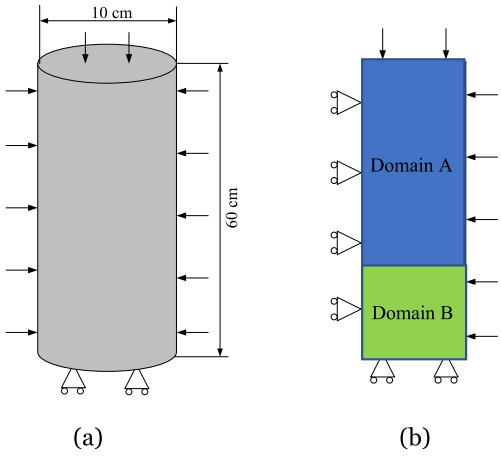

Fig. 7. (a) Laboratory specimen and the experimental boundary conditions, (b) the model domain and the assigned boundaries for validating the model against the coal permeability data.

Table 3
Material parameters used in validation test against experiment.

Parameters	Value
Young's modulus of coal, E (GPa)	1.8
Poisson's ratio, ν (−)	0.3
Initial permeability, k_{f0} (m2)	A: 5.1e-15 B: 6.1e-17
Initial matrix porosity, n_m (−)	0.059
Initial fracture porosity, n_f (−)	0.017
Density of coal, ρ_c (kg/m3)	1388
Viscosity of gas, μ_g (Pa•s)	1.1e-5
Effective diffusion coefficient, Dm (m2/s)	1.2e-11
Langmuir volume constant for CO2, c_L (mol/kg)	0.64
Langmuir pressure for CO2, b_L (MPa-1)	0.71
Rate constant for desorption, γd, s-1	1.5e-3
Formation temperature, T (K)	298
Fracture compressibility at reference state, C_{f0} (MPa-1)	0.086
Fracture compressibility change rate, α (MPa-1)	0.15
Weakening coefficient for CO2, γ (−)	0.92
Space of coal matrix block, a, (m)	A: 3.2e-3, B: 4.1e-3

Note: A, B denote domain A and.

4.1.2. Numerical validation of the pressure measurements of he and CO_2 single species injection on EMB coal

The pressure measurements were validated using the numerical model (model development is described in the supplementary section). The core sample used for experimental measurement is cylindrical, as shown in Fig. 7a. Due to the axial symmetry, the cylindrical coal sample is simplified as a 2D model for numerical simulation, as shown in Fig. 7b. According to the experimental conditions, the boundary conditions required for this validation simulation are shown in Fig. 7a. For gas flow, a zero-flux boundary is applied to the right and left boundaries of the domain. The constant flux boundary is assigned to the top surface, and the outlet pressure is used as the outlet boundary condition. For coal deformation, a vertical constraint is applied to the outflow boundary while a constant confining stress is applied to the right and inflow boundaries. The left side of the model is fixed horizontally. The initial pressure for both the fracture and matrix continua is 0.01 MPa. The parameters that are used in this test are listed in Table 3. These parameters are obtained from experimental measurements or matching permeability data. Separate adsorption kinetics were performed, which have been used for determining the Langmuir constants for CO_2 adsorption (Masum et al., 2023; Sadasivam et al., 2022). The parameters for the stress dependent permeability model, including fracture compressibility, the change rate of fracture compressibility caused by

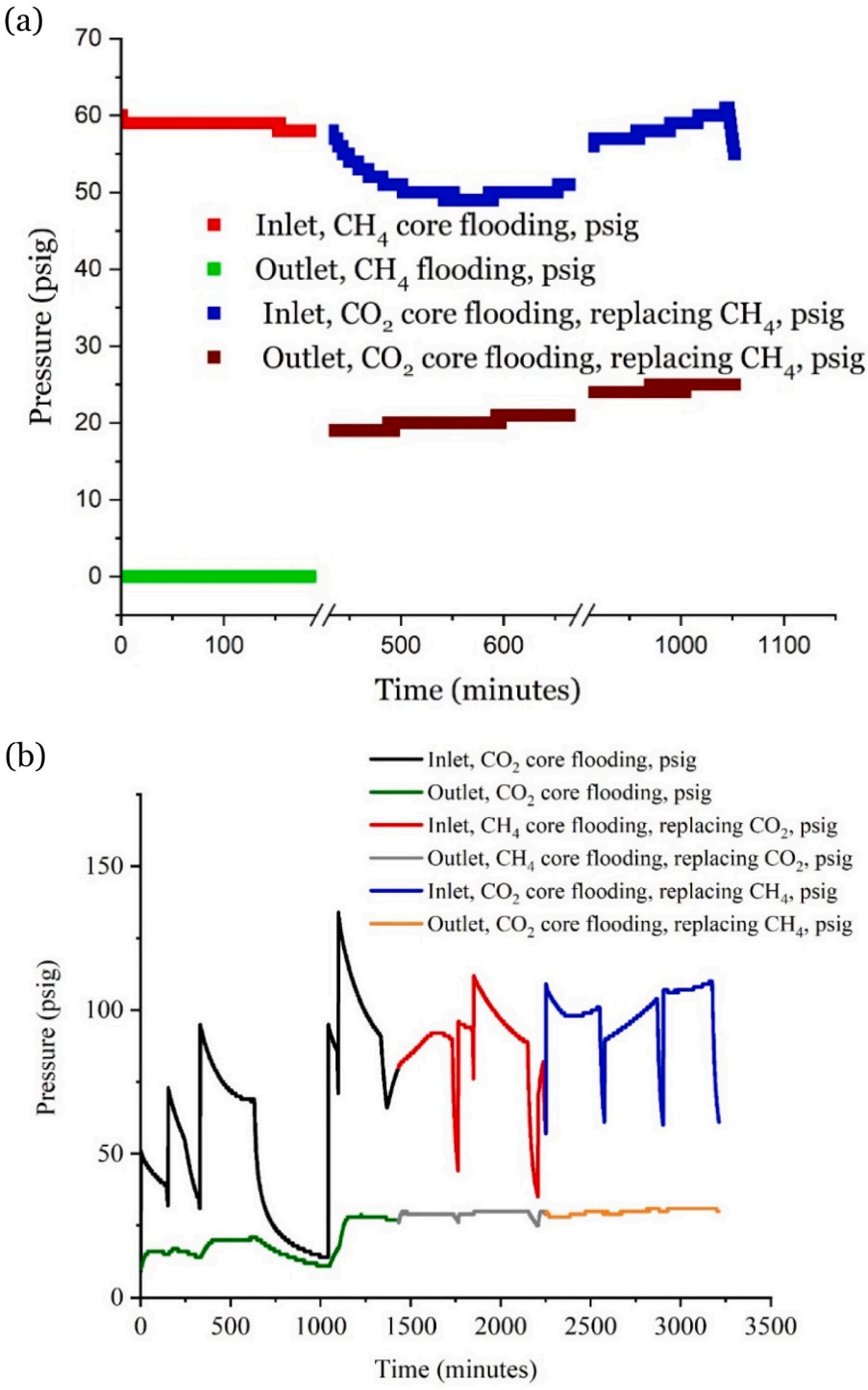

Fig. 8. Inlet and outlet gas pressures (psi) of CH4 flooding and CO2 flooding to replace the CH4 on (a) EMB and (b) ZM coal cores at confining pressure of 1450 psi, flowrate of 1.67×10^{-08} m^3/s and outlet or downstream pressure set at 25 to 30 ± 2 psi. Please note that the pressure unit at y-axis 'psig' represents gas pressure in 'psi' unit.

effective stress, and the weakening coefficient due to CO_2-coal interaction, are unknown. To determine the values of these parameters, the following two steps are adopted: 1) application of permeability data on He to determine the fracture permeability and fracture compressibility; 2) application of permeability data on CO_2 to determine the weakening coefficient of the permeability model.

It was observed from laboratory tests that the pressure difference between the inlet and pressure taps (dp1 and dp2) is slight, that is, the gas pressure at the inlet and pressure taps are close values. It can be inferred that the permeability from the inlet to dP2 should be so high that there is a low-pressure gradient. To capture the heterogeneity of a coal sample, the sample is separated into two parts, domain A and domain B, as shown in Fig. 7b. The fitting initial permeabilities under the unstressed state for both domains are 5.1 mD and 0.061 mD, respectively. The average permeability is 2.58 mD. The estimated fracture compressibility is 0.086 MPa^{-1}, and the weakening coefficient is 0.92. The fitting size of a matrix block is 3.2 and 4.1 mm for domain A and domain B, respectively. The comparison results of gas pressure

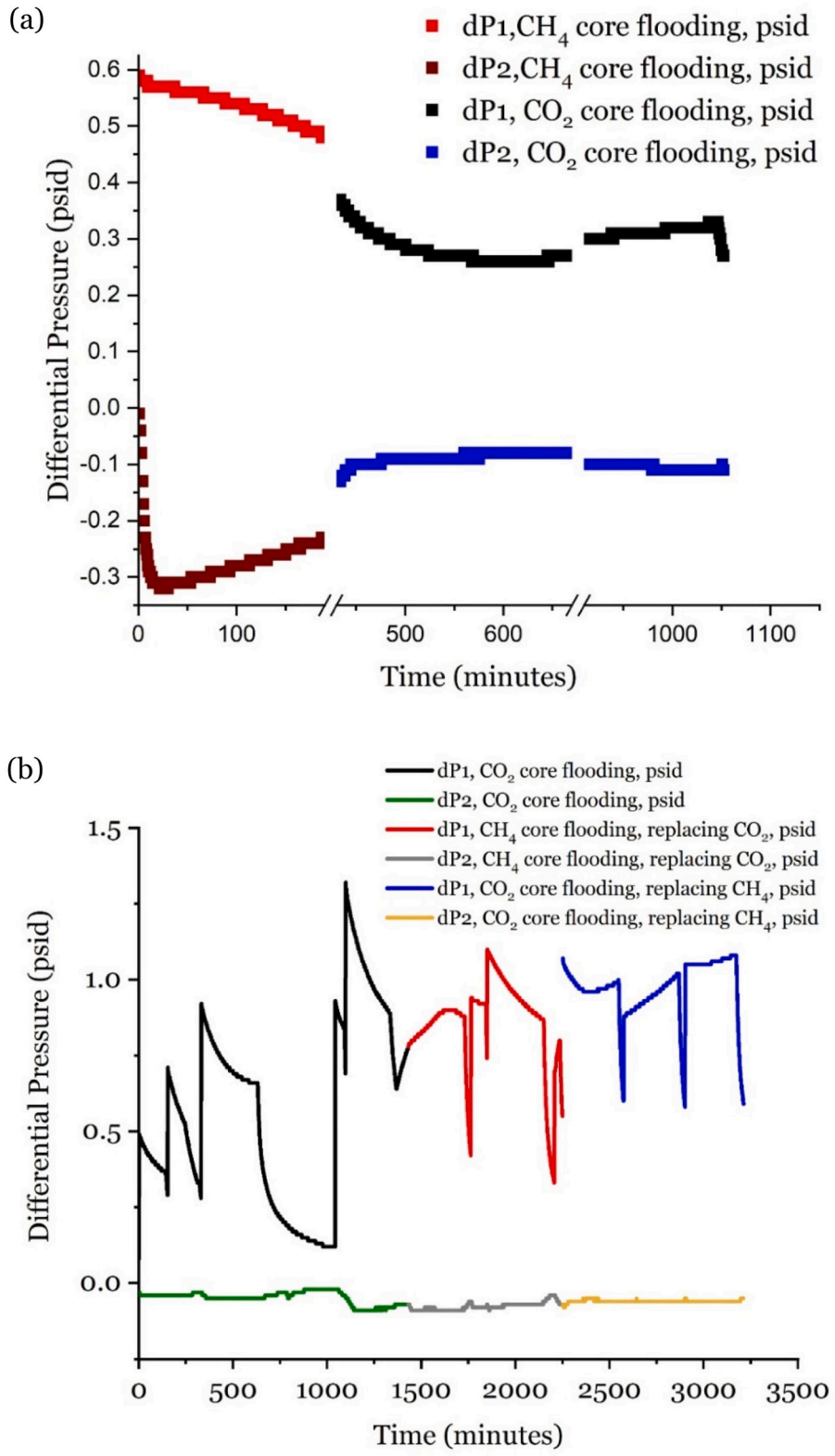

Fig. 9. dP1 and dP2 differential pressures (psi) of CO2-CH4 core flooding with (a) EMB and (b) ZM coal. Please note that the pressure unit at y-axis 'psid' represents differential pressure in 'psi' unit.

predicted by the model and experimental measurements are shown in Figs. 5 and 6.

4.1.3. Pressure measurements of the core flooding experiments

The core flooding tests were aimed at determining the CH4 replacement efficiency by CO2, the relative permeabilities of CO2 and CH4 when they dispersed within the coal core, and the dependency of the core lengths on the random permeability measurements of the coal cores. Fig. 8 depicts the inlet and outlet pressures developed during the core flooding experiments conducted on the EMB and ZM samples. The

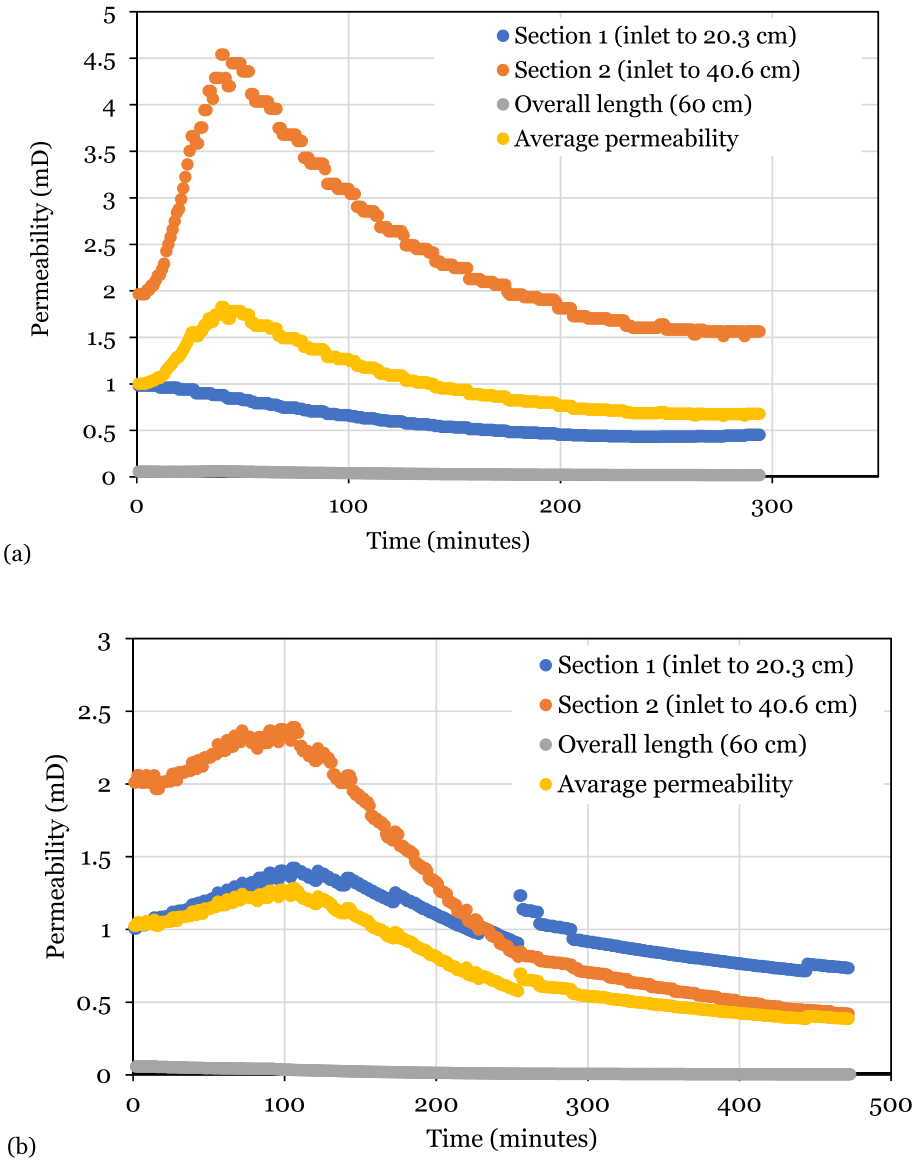

Fig. 10. Shows the He permeability data in millidarcy (mD) calculated using Eq. (1). (a) 1088 psi and (b) 1450 psi confining pressures, 1 mL/min flowrate outlet or downstream pressure at 25 ± 2 psi and 298.15 K. Corresponding pressure measurements and numerical model validation are presented in Section 4.1.

CO2-CH4 core flooding experiments were more related to the ZM samples with a perspective on CO2-ECBM.

The constant outlet pressure (25 to 30 ± 2 psi) was set up to replicate the constant tangential pore pressure as expected in coal seams (Fig. 8 a and b). The stable back pressure measurements are shown in Fig. 8a after 700 min for EMB and in Fig. 8b after 1000 min for ZM coal. This outlet set value is crucial for permeability calculations because if the gas leaves the core without any backpressure, the permeability calculation is entirely dependent on the outlet pressure and preferential pathways. To avoid this scenario, the measurements along the core length (inlet, outlet, and dP1 and dP2) must be carried out with a backpressure setup to mimic the field conditions. The CH4 displacement efficiency and the CO2 and CH4 permeability values that were calculated from the pressure measurements taken during the core flooding experiments are discussed in the subsequent sections.

During the CO2 injection, the pressure dropped at the inlets of both coal samples (Fig. 8a and b, blue lines). This shows that the CO2 was adsorbed and CH4 was displaced from the fractures. The gas replacement was detected using gas analysers that measured the volume composition of the gas released from the outlet. Fig. 9 shows the differential pressures at 20.3 cm (dP1) and at 40.6 cm (dP2) of the cores. These differential pressure values were converted to absolute pressures for the corresponding measurement points. For example, dP1 is the difference between inlet pressure (P_{in}) and absolute pressure at 20.3 cm. The absolute pressure values are substituted as in Eq. (1) to calculate the permeability of the specific lengths of core Sections 1 (20.3 cm) and Section 2 (40.6 cm). The inlet (P_{in}) and outlet pressure (P_o) values shown in Fig. 8 were used in Eq. (1) to calculate the permeability for the overall length of the core sample.

The dP1 follows the same pattern as the values of the inlet pressure, and the low-pressure differentials showed that the inlet pressures used in this study caused the coal to swell less at a high confining pressure of 1450 MPa (Fig. 9a and b). The stable line of dP2 shows that Section 2 reached similar pressure values as dP1 and followed a similar pattern but reflected a much lower or no differential from dP1.

4.2. Permeability measurements

4.2.1. He and CO2 permeability of EMB coal

The pressure measurements at inlet, outlet, dp1 and dp2 were used in

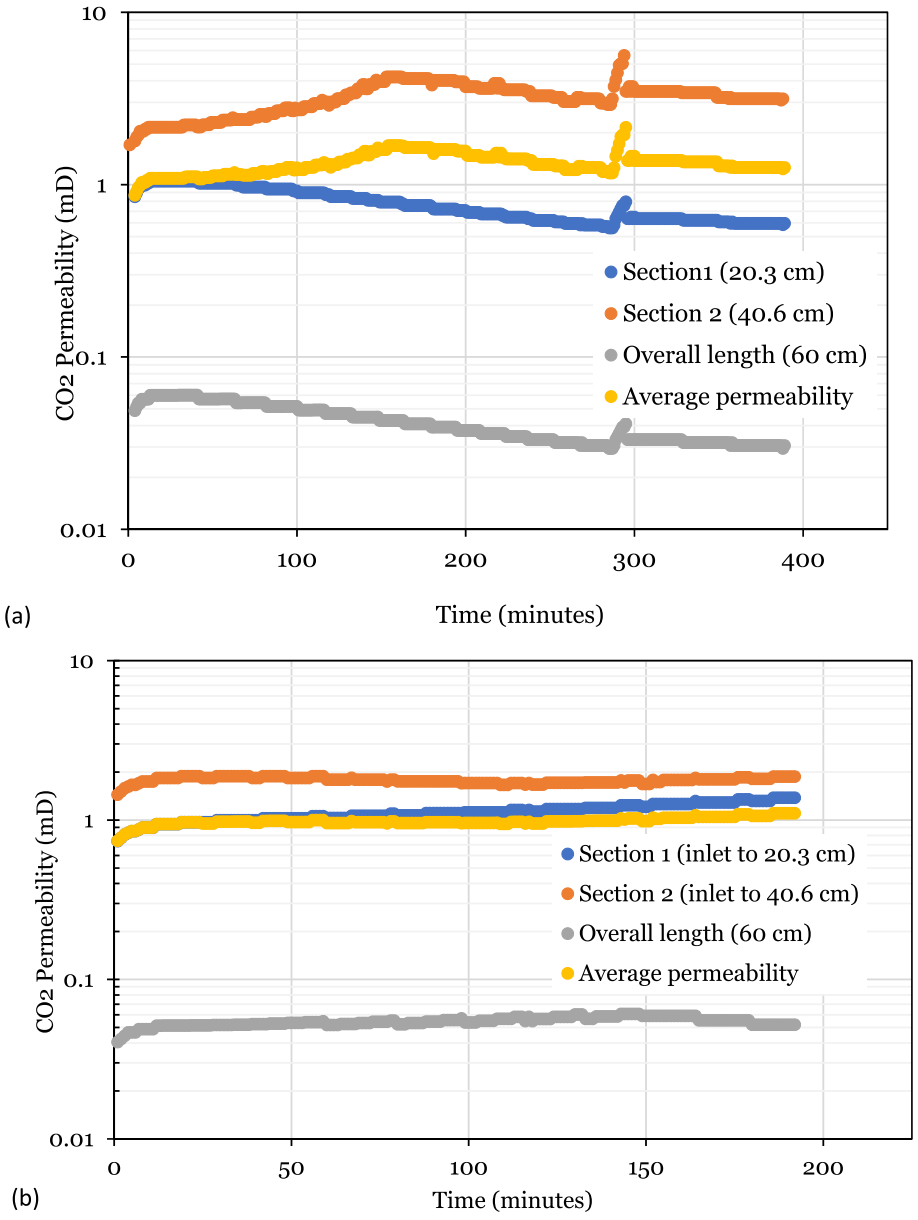

Fig. 11. CO_2 permeability evolution at different lengths of the intact core sample under (a) 1088 psi and (b) 1450 psi confining pressures, 1 mL/min flowrate outlet or downstream pressure at 25 ± 2 psi and 298.15.

Eq. (1) to obtain the permeability values. Section 4.1 presents the pressure measurements and numerical model validation along the length of the core which showed the time steady state condition attained. Fig. 10 depicts the He permeability data along the core length as well as the average permeability for the confining pressures of 1088 and 1450 psi. Under 1088 psi confining pressure, the permeability varied from 0.45 mD to 0.98 mD up to the first 20.3 cm (Section 1) of the length from the inlet (Fig. 10a). However, up to 40.6 cm length of the core sample (Section 2), the permeability ranged from 1.56 mD to 4 mD, and for the overall length the permeability ranged from 0.017 mD to 0.056 mD. The average permeability under 1088 psi confining pressure varied between 0.68 mD and 1.79 mD (Fig. 10a). Please note that the calculated permeability values, accounting overall length of the core, are much smaller than that of the segment permeability or average permeability. Since permeability of such large, intact coal cores have not been measured in previous studies (literatures), a plausible explanation can be adopted from permeability measurements of large shale or sandstone cores. The series bed or linear bed analysis (e.g., liner permeability variation along the core length) is used to explain relative permeability and average permeability of large sandstone or shales samples (Glover, 2008; Chen and DiCarlo, 2016). In their studies, Glover (2008) and Chen and DiCarlo (2016) observed that overall permeability was much lower than the measured permeability at each section for sandstone or shale cores.

The advantage of the current study is that it measures gas pressures at the pressure-taps roughly matching the rules of linear bed analysis used for sandstone or shale. For example, following (Glover, 2008; Chen and DiCarlo, 2016):

$$(p_i - p_o) = (dP1) + (dP2) + (Pressure\ at\ dP2 - p_o) \quad (2)$$

Substituting Equation with experimentally measured values of current study, at 50 min, the inlet, outlet pressure values from Fig. 5a and dP1 and dP2 from Fig. 6a resulted as 27 psid = 0.45 psid −0.28 psid +26.83 psid = 27 psid. It shows that the pressure drops, and the permeability is influenced by the lower permeability zone or influenced by the obstructed flow associated with the heterogeneous nature of the

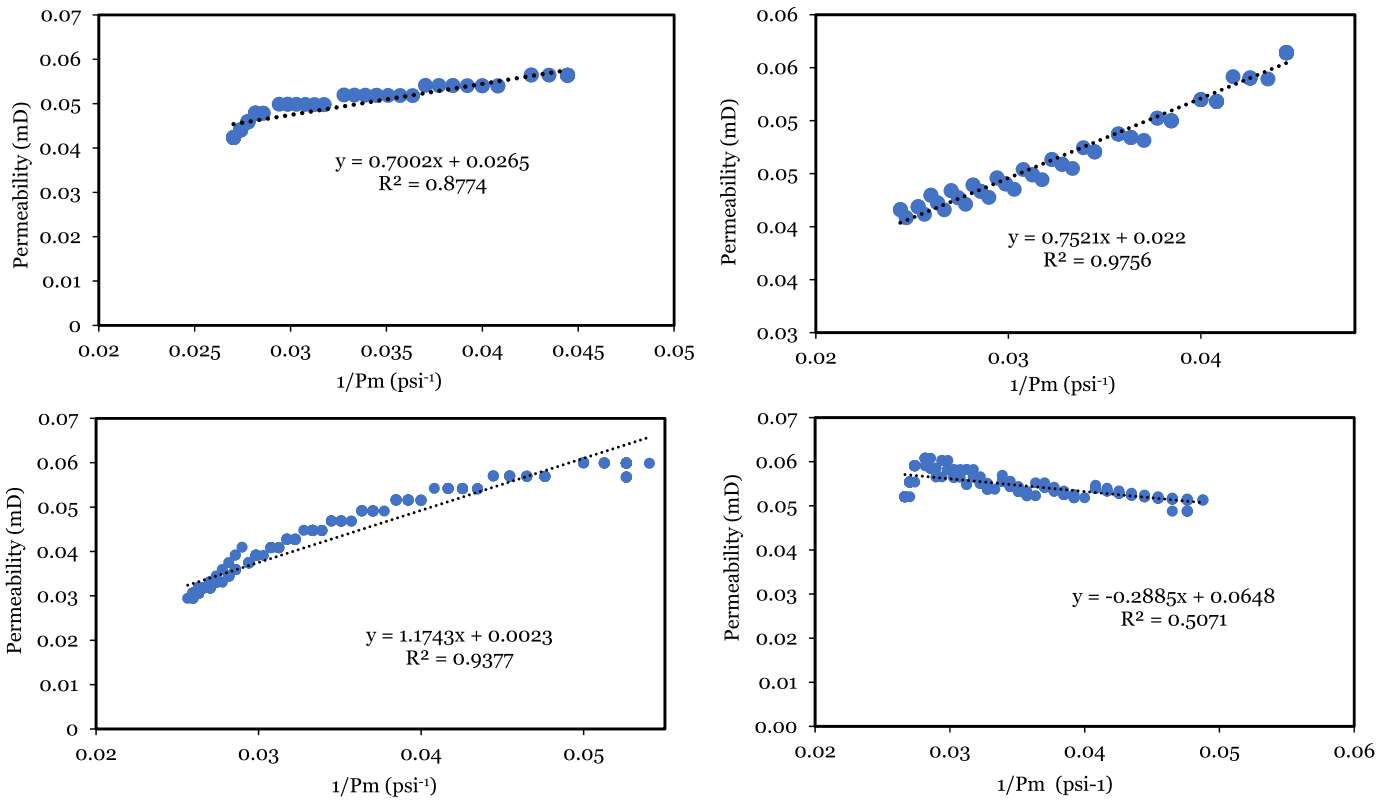

Fig. 12. Apparent (CO_2 gas) permeability versus mean pore pressure plots to obtain Klinkenberg intrinsic permeability (k_∞) at (a) 1088 psi and (b) 1450 psi confining pressures for He, (c) 1088 psi and (d) 1450 psi confining pressures for CO_2.

large core sample. The overall permeability reflects the random variation of the permeability within each section. Permeability of fractured porous media is random rather than uniform throughout a large sample. This effect might not be captured by powdered samples or reconstructed samples from small coal aggregates.

Under 1450 psi confining pressure, the permeability was ranging from 0.71 mD to 1.42 mD up to the core length of 20.3 cm (Section 1; Fig. 10b). The permeability of the core was ranging from 0.41 mD to 2.39 mD up to 40.6 cm (Section 2; Fig. 10b) and for the overall length resulted in 0.0035 mD to 0.056 mD (Fig. 10b). The average permeability under 1450 psi confining pressure varied from 0.38 to 1.28 mD. As mentioned previously that the core samples which are being tested in this study are significantly larger than the samples considered in previous studies (or existing literatures), a direct comparison of He permeability values cannot be obtained. However, some qualitative comparison can be performed. The permeability values measured in this test are in-line with literature data of similar experimental conditions. For example, Meng et al. (2021) reported that the He permeability varied from 0.00001 to 0.0037 mD at gas pressures of 21.75 psi to 101 psi under confining pressures ranging from 601 psi to 15,519 psi. Wang et al., 2019 estimated He permeability of 0.001 mD at 12 MPa (1745 psi) confining pressure and gas pressure of 6 MPa (870 psi).

Fig. 11 shows the CO_2 permeability evolution results along the core length and the average permeability values for 1088 and 1450 confining pressures. Under 1088 psi confining pressure (Fig. 11a), the permeability in Section 1 (inlet to 20.3 cm of the core) varied from 0.59 mD to 1.04 mD. In Section 2 (inlet to 40.6 cm of the core) the permeability varied from 1.7 mD to 5.6 mD. For the overall length of the core the measured permeability varied from 0.03 mD to 0.06 mD. Under 1450 psi confining pressure (Fig. 11b), the Section 1 permeability ranged from 0.74 mD to 1.38 mD. In Section 2, the permeability varied between 1.44 mD and 1.88 mD. For the overall length the permeability ranged from 0.04 mD to 0.059 mD for 1450 psi confining pressures.

The results shows that the confining pressure influences the permeability. For a high volatile bituminous coal, reported permeability variation ranged from 0.428 mD to 1.374 mD at 452 psi confining pressure (Li et al., 2014). Previous literature that studied small cores and reconstructed samples reported permeability values between 0.02 mD to 0.045 mD at gas pressures 3 MPa and confining pressure of 6 MPa (870.2 psi) (Wei et al., 2019), and from 0.6 mD to 0.1 mD at 2 MPa to 6 Mpa gas pressure and 10 Mpa (1450.38 psi) confining pressure (Kumar et al., 2015). For a longer core made using compacted pulverised coal (20.3 cm diameter and 80 cm length), De Silva and Ranjith (2013) reported permeability variation between 0.001 mD to 10 mD at gas injection pressures between 0.1 MPa to 4 MPa. The current study correlated with previous works and also demonstrated the variation of permeability along the core length for a large intact core of 60 cm long and 9.9 cm diameter. The study also suggests that permeability measurements based solely on inlet/outlet pressures may not accurately represent permeability within cores, which is more relevant to the field condition of CO2 storage in coal seams.

The intrinsic permeability (k_∞) of the single species flow was calculated using Klinkenberg equation (Eq. 2) to include the gas slippage effect (API RP 40, 1998; Klinkenberg, 1941. The intrinsic permeability (k_∞) and gas slippage factor (*b*) for the mean pore pressure (p_m) values ($p_m = \frac{(p_i+p_o)}{2}$) were obtained for the single species flow from the plots in Fig. 11.

$$k_g = k_\infty\left(1+\frac{b}{p_m}\right) \tag{3}$$

The estimated Klinkenberg permeability for He was 0.0265 mD for 1088 psi (Fig. 12a) and 0.022 mD for 1450 psi (Fig. 12b) confining pressures experimental conditions. The *b* (gas slippage factor) values were 26.42 psi and 34.19 psi, respectively (average pore pressure values for confining pressure of 1088 psi were ranging from 19 to 38 psi and 22 psi to 103 psi for confining pressure of 1450 psi).For CO2, the

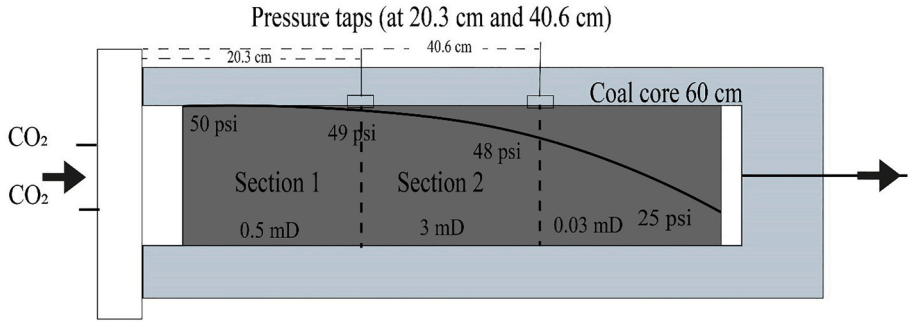

Fig. 13. Series bed analysis Pressure drops and apparent permeability profile along the core length for confining pressure of 1088 psi.

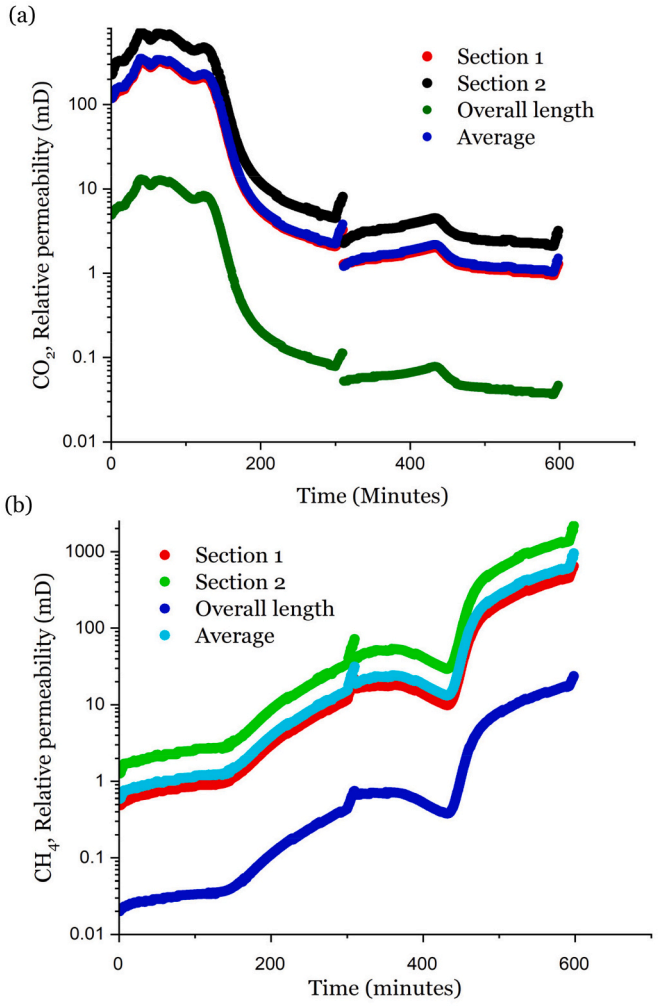

Fig. 14. (a) CO2 and (b) CH_4 permeabilities of EMB coal core during core flooding experiments.

(Klinkenberg permeability) k_∞ = 0.0023 mD for 1088 psi (Fig. 12c) confining pressures and b (gas slippage factor) value of 510.6 psi (Fig. 12c) for mean pore pressure values ranging from 19 to 38.5 psi. At higher confining pressure, the permeability values were almost stable for varying pore pressure. Therefore, it was not possible to calculate the intrinsic permeability for experiments conducted at 1450 psi confining pressure (Fig. 12d).

Fig. 13 shows the linear bed series analogy and the gas permeability of the sections virtually made based on the pressure tap locations. The permeability values shown in the figure are calculated using the stable pressure values observed at the pressure transducers. The average permeability value was in the range of 1.74 mD for the 50-psi injection pressure and 25 psi outlet pressure and 1088 psi confining pressure. The image depicts the linear bed analysis discussed above.

4.2.2. CO2 and CH4 permeability of EMB and ZM coals during core flooding

The partial pressures of CH4 and CO2, calculated from the pressure values measured at the inlet and outlet, dP1 and dP2, were used in Eq. (1) to calculate the CO2 and CH4 permeabilities of EMB and ZM coal cores. The 60 cm core was theoretically sectioned using the locations of the two pressure taps, dP1 and dP2 (as shown in Figs. 3 and 13).

Fig. 14a shows the CO2 permeability of the EMB coal along the lengths of the core. As CO2 replaced CH4, the permeability values in Section 1 decreased from 717 mD to 3 mD. At the same time, Section 2 showed the permeability had stabilised at approximately 1.5 mD, starting at 353 mD. The CO2 permeability values for overall length have stabilised at 0.05 mD from 13 mD. The average permeability value for the core flooding experiment ranged from 298 mD to 1 mD. As the CO2 permeated through the coal by driving out the CH4, the permeability values showed a decreasing trend, and the average permeability value was stable around 1 to 2 mD for the given conditions (contained pressure of 1450 psi, flow rate of 1 mL/min, and back pressure of 25 psi). The average permeability values were reproducible from the single species core flooding experiments (CO2 permeability of EMB coal = 0.7 to 1.1 mD under 1450 psi confining pressure; Fig. 11).

The CH4 permeability of EMB coal shows an opposite trend to the CO2 permeability measurement (Fig. 14b). As the CO2 displaced the CH4, the permeability of the CO2 increased. Section 1 showed permeability values ranging from 0.48 mD to 702 mD. Section 2 showed permeability values ranging from 1.25 mD to 2180 mD, whereas the overall length of the coal exhibited permeability values ranging from 0.019 mD to 23.57 mD. The average permeability of the measured CH4 permeability values along the core samples ranged from 0.66 mD to 950 mD. The increasing trend in CH4 permeability and the opposite trend observed in CO2 permeability shows the coal's affinity towards CO2 and sweeping ability of CO2 as the CH4 driven out of the coal core.

Fig. 15a shows the CO2 permeability measurements of the ZM coal cores. The average CO2 permeability ranged from 1.5 mD to 0.003 mD in single species flooding experiments. During the CH4 injection to the core saturated with CO2, the CO2 permeability values showed an increasing trend (Fig. 15a). Section 1 of the core exhibited permeability values ranging from 0.006 mD to 0.15 mD. Section 2 showed 0.5 mD to 5.5 mD, whereas the overall length of the core sample showed CO2 permeability values of 0.02 to 0.04 during CH4 injection. The average CO2 permeability values were calculated at 0.2 to 1 mD for the ZM coal during CH4 injection. The hills in the plots represent the pressure buildup shown for the Section 1 of the core (Fig. 8) and the gas gradually permeate the rest of the coal sections.

During the CO2 injection to replace the CH4, the CO2 permeability values showed a decreasing trend. The average permeability value

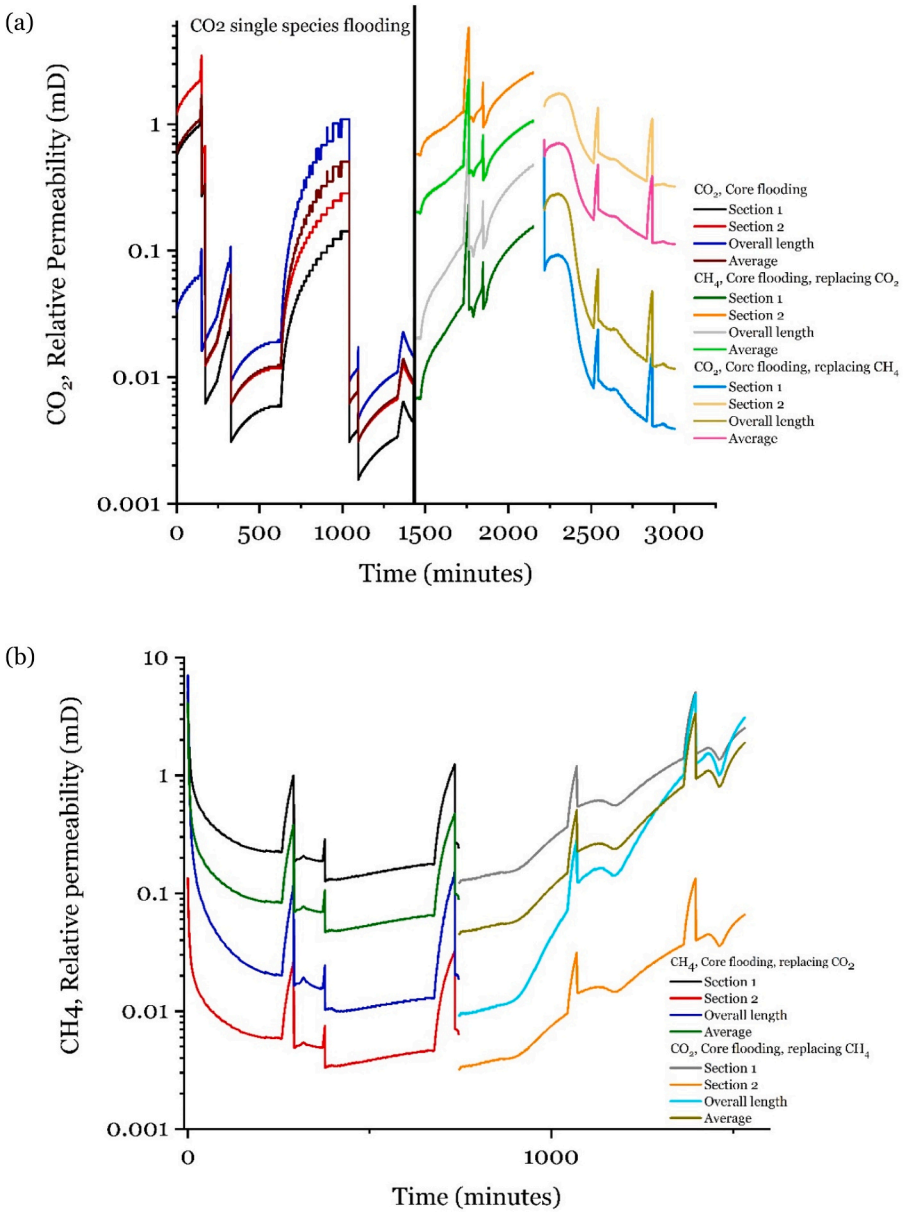

Fig. 15. (a) CO2 and (b) CH_4 permeabilities of ZM coal core during core flooding experiments.

ranged from 0.75 to 0.1. The CO2 permeability of Section 1 decreased from 0.6 mD to 0.003 mD. Section 2 decreased from 1.7 mD to 0.3 mD. The permeability values measured for the overall length of the core showed permeability values of 0.3 mD to 0.01 mD. Comparatively, the CO2 permeability values measured along the core sample were comparable to the previously published computed or estimated values of 3 mD to 1.5 mD for the Upper Silesian Coal Basin (McCants et al., 2001). However, the average CO2 permeability values measured during the two species flows of the current study were much lower than the computed values reported for samples from 116 to 1396 m [43]. ZM coal exhibited much lower permeability values than EMB coal. The primary reason the EMB coal is more fractured than the ZM coal is that it provides preferential CO2 pathways.

The CH4 permeability values were measured during the CH4 and CO2 injections (Fig. 15b). During the CH4 injection, the permeability values showed a decreasing trend, and vice versa for the CO2 injection. For CH4 injection, Section 1 showed CH4 permeability values of 7 mD to 0.17 mD. Section 2 had permeabilities ranging from 0.13 mD to 0.004 mD, while the overall length of the core had permeabilities ranging from 0.77 to 0.12 mD. The average permeability values during the CH4 injection to replace the CO2 were 4.1 mD to 0.06 mD.

During the CO2 injection, Section 1 showed CH4 permeability values of 0.12 mD to 5 mD. Section 2 showed a permeability of 0.003 mD to 0.12 mD, whereas the overall length of the core showed a permeability of 0.009 to 3 mD. The average CH4 permeability values during the CO2 injection to replace the CH4 were 0.045 mD to 1.89 mD.

4.3. CO2-CH4-CO2 displacement

Fig. 16a and b display the volume fractions of CO2 and CH4 at the outlet measured during the flooding experiments. In the beginning, the EMB coal was flooded with CO2, and CH4 was injected to determine the sweep efficiency. For EMB coal, 77% CO2 was measured at the outlet when the CH4 was injected at a rate of 1 mL/min. Due to the convection and dispersion of the gases, the CH4 concentrations reach the outlet within 30 min. After 465 min of injection, CH4 reached a maximum volume fraction of 95.02% at the outlet by removing 93.72% of the CO2 (Fig. 16a). Then the adsorbed CH4 was replaced by CO2 (injection rate

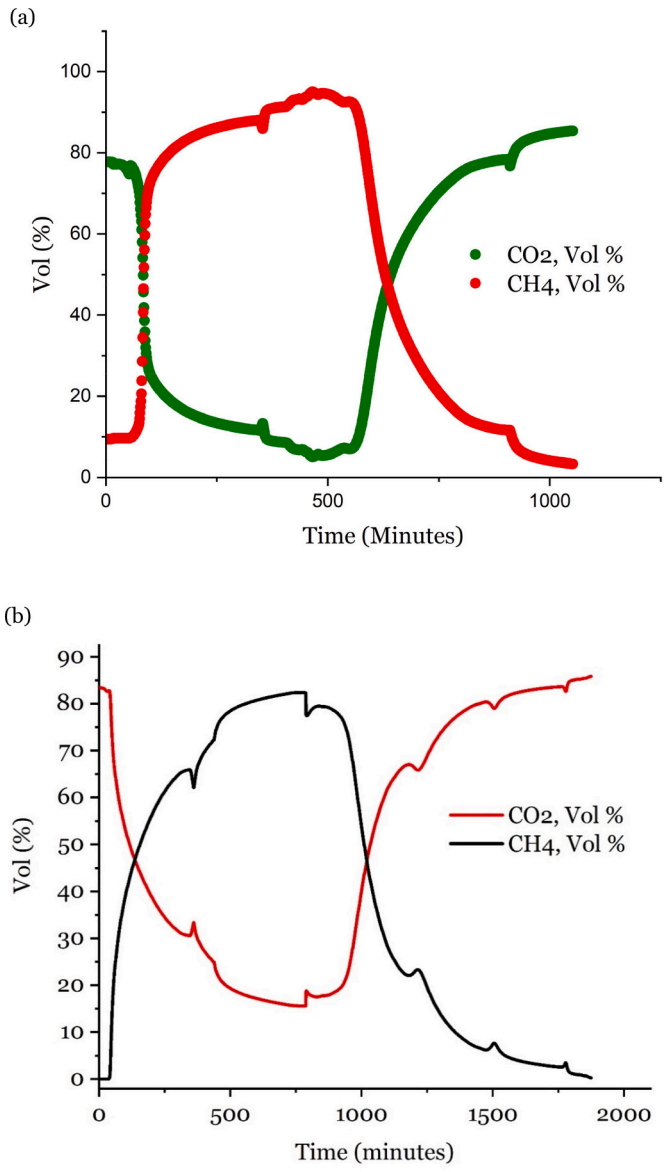

Fig. 16. CH_4-CO_2_CH_4 gas exchange core flooding experiment gas composition measured at outlet for (a) EMB and (b) ZM coal cores.

of 1 mL/min). The efficiency of CH4 removal by CO2 was 96.5%, slightly higher than the CO2 removal efficiency by CH4 (93.72%). This behaviour was more pronounced in the ZM samples (Fig. 16b).

The ZM samples were more relevant for the core flooding experiments as the coal seam has the potential for CO2-ECBM. Initially, the core was flooded with CO2, and the volume fraction of CO2 measured at the outlet was about 83.42%. After injecting CH4 for 789 min at a flow rate of 1 mL/min, the volume fraction of CO2 at the outlet was about 15.59%. The CO2 removal efficiency of CH4 was about 81.31% (ie., 81.31% of CO2 removed from the core) (Fig. 16b). In the contract, the CH4 removal efficiency by CO2 was about 99.7%, almost driving out all the CH4 from the coal. The volume fractions measured in these experiments were used to calculate the partial pressures of the CO2 and CH4 gases to determine the relative permeabilities of the two species during the core flooding experiments. The complete CH4 sweep efficiency of CO2 has previously been observed in a few studies with constructed coal cores (Niu et al., 2020; Ranathunga et al., 2017; Shi et al., 2008; Zhang and Ranjith, 2019).

5. Conclusions

The following conclusions are drawn from the experimental investigations carried out to address the CO2 injection into shallow level coal seams.

1. The single species flow experiments conducted on EMB coal showed that the average He permeability of the EMB coal varied between 0.68 and 1.79 mD under 1088 psi (or 7.5 MPa) confining pressure and between 0.38 and 1.28 mD under 1450 psi (or 10 MPa) confining pressure. The calculated theoretical or empirical intrinsic permeability was 0.0265 mD and 0.022 mD respectively. The average CO_2 permeability of the EMB coal varied between 0.86 and 1.68 mD under 1088 psi confining pressure and between 0.7 and 1.1 mD under 1450 psi confining pressure. The calculated theoretical/empirical intrinsic permeability was 0.0023 mD for 1088 psi (7.5 MPa) confining pressure condition. The pressure measurements conducted on the EMB coal indicated that the low-pressure injections create more residential time and allow the CO2 to permeate and adsorb in pores.
2. The permeability of CO2 observed during the single species (CO2) flow was 0.003 mD to 1.5 mD for ZM samples, which was comparable with the predicted values from previous studies. However, the ZM coal samples exhibited low average CO2 permeability of 0.1 mD to 0.75 mD (averaged along the core length) during the two species flow (CO2 & CH4) during the CO2 flooding to replace CH4. The results indicated a decreasing trend in CO2 permeability and increasing CH4 permeability during CO2 injection. The observation indicated CO2 adsorption and CH4 displacement.
3. Both coals, EMB and ZM, showed favourable CH4 displacement efficiencies of 96.5% and 99.7%, respectively. The ZM coal from 900 m depth had a high probability of CH4 presence, and the results observed in the current study showed the potential for CO2-ECBM prospects.
4. The CO2 permeability measurements made at 20.3 cm, 40.6 cm, and 60 cm of the core length showed the variation of the CO2 and CH4 permeabilities, indicating the nature of the heterogeneous pore structure within the coal block. Previous experimental studies considered small core samples or large constructed samples using pulverised coal samples. The dependency of the core length for the laboratory experiments is more pronounced in the results obtained in the current study to replicate the in-situ conditions, which recommends large-scale ex-situ tests using intact coal blocks.
5. EMB coal showed CO2 permeability of 1 to 2 mD during the CO2 core flooding by exchanging CH4. The results reflect that the EMB coal is more fractured than the ZM coal. The two species flow experiments indicated that EMB coal which is from shallow level coal seam is in favour of CCS operations in terms of permeability and adsorption characteristics.
6. The numerical modelling used in the current study was well fitted with the experimental values. The model can be extended to predict the pressure measurements and permeability values to design and predict the pre and post injection parameters.

CRediT authorship contribution statement

Maram Almolliyeh: Conceptualization, Methodology, Data curation, Investigation, Visualization, Formal analysis, Writing – review & editing. **Sivachidambaram Sadasivam:** Conceptualization, Methodology, Data curation, Investigation, Visualization, Formal analysis, Writing – review & editing. **Min Chen:** Methodology, Validation, Formal analysis, Writing – review & editing. **Shakil Masum:** Conceptualization, Project administration, Formal analysis, Writing – review & editing. **Hywel Rhys Thomas:** Funding acquisition, Project administration, Resources, Writing – review & editing.

Declaration of Competing Interest

The authors declare that they have no known competing financial interests or personal relationships that could have appeared to influence the work reported in this paper.

Data availability

Data will be made available on request.

Acknowledgement

The research was conducted as part of the "Establishing a Research Observatory to Unlock European Coal Seams for Carbon Dioxide Storage (ROCCS)" project. The ROCCS project has received funding from the Research Fund for Coal and Steel under Grant Agreement No. 899336. The financial support is gratefully acknowledged. The authors would like to thank Malcolm Seaborne, Technician, School of Engineering, Cardiff University for the technical support.

Appendix A. Supplementary data

Supplementary data to this article can be found online at https://doi.org/10.1016/j.coal.2023.104376.

References

API Report 40, 1998. Recommended Practice for Core Analysis Procedure, Second edition ed. American Petroleum Institute Publishing Services, 1220 L Street, N.W., Washington, D.C, p. 20005.
Chen, X., DiCarlo, D.A., 2016. A new unsteady-state method of determining two-phase relative permeability illustrated by CO2-brine primary drainage in berea sandstone. Adv. Water Resour. 96, 251–265.
Chen, S., Tang, D., Tao, S., Xu, H., Zhao, J., Fu, H., Ren, P., 2018. In-situ stress, stress-dependent permeability, pore pressure and gas-bearing system in multiple coal seams in the Panguan area, western Guizhou, China. J. Nat. Gas Sci. Eng. 49, 110–122.
Cui, X., Bustin, A.M.M., Bustin, R.M., 2009. Measurements of gas permeability and diffusivity of tight reservoir rocks: different approaches and their applications. Geofluids 9, 208–223.
De Silva, P.N.K., Ranjith, P.G., 2013. Advanced core flooding apparatus to estimate permeability and storage dynamics of CO2 in large coal specimens. Fuel 104, 417–425.
Gensterblum, Y., Ghanizadeh, A., Krooss, B.M., 2014. Gas permeability measurements on Australian subbituminous coals: Fluid dynamic and poroelastic aspects. J. Nat. Gas Sci. Eng. 19, 202–214.
Glover, P., 2008. Formation evaluation. Chapter 6 Single phase permeability. Course notes. Chapter6.PDF. leeds.ac.uk.
Hadi Mosleh, M., Sedighi, M., Vardon, P.J., Turner, M., 2017. Efficiency of carbon dioxide storage and enhanced methane recovery in a high rank coal. Energy Fuel 31, 13892–13900.
Harpalani, S., Chen, G., 1997. Influence of gas production induced volumetric strain on permeability of coal. Geotech. Geol. Eng. 15, 303–325.
Hol, S., Spiers, C.J., Peach, C.J., 2012. Microfracturing of coal due to interaction with CO2 under unconfined conditions. Fuel 97, 569–584.
Klinkenberg, L.J., 1941. The permeability of porous media to liquids and gases. drilling and production practice. Am. Pet. Inst. 200–213.
Kumar, H., Elsworth, D., Liu, J., Pone, D., Mathews, J.P., 2015. Permeability evolution of propped artificial fractures in coal on injection of CO2. J. Pet. Sci. Eng. 133, 695–704.
Larsen, J.W., 2004. The effects of dissolved CO2 on coal structure and properties. Int. J. Coal Geol. 57, 63–70.
Li, D., Liu, Q., Weniger, P., Gensterblum, Y., Busch, A., Krooss, B.M., 2010. High-pressure sorption isotherms and sorption kinetics of CH4 and CO2 on coals. Fuel 89, 569–580.
Li, Y., Tang, D., Xu, H., Meng, Y., Li, J., 2014. Experimental research on coal permeability: the roles of effective stress and gas slippage. J. Nat. Gas Sci. Eng. 21, 481–488.
Liu, J., Chen, Z., Elsworth, D., Miao, X., Mao, X., 2011. Evolution of coal permeability from stress-controlled to displacement-controlled swelling conditions. Fuel 90, 2987–2997.
Liu, C.J., Wang, G.X., Sang, S.X., Gilani, W., Rudolph, V., 2015. Fractal analysis in pore structure of coal under conditions of CO2 sequestration process. Fuel 139, 125–132.
Liu, Z., Liu, D., Cai, Y., Pan, Z., 2020. Experimental study of the effective stress coefficient for coal anisotropic permeability. Energy Fuel 34, 5856–5867.
Liu, Y., Lebedev, M., Zhang, Y., Wang, E., Li, W., Liang, J., Feng, R., Ma, R., 2022. Micro-cleat and permeability evolution of anisotropic coal during directional CO2 flooding: an in situ micro-CT study. Nat. Resour. Res. 31, 2805–2818.
Masum, S.A., Sadasivam, S., Chen, M., Thomas, H.R., 2023. Low subcritical CO2 adsorption–desorption behavior of intact bituminous coal cores extracted from a shallow coal seam. Langmuir 39, 1548–1561.
Mazumder, S., Wolf, K.H., 2008. Differential swelling and permeability change of coal in response to CO2 injection for ECBM. Int. J. Coal Geol. 74, 123–138.
Mazumder, S., Scott, M., Jiang, J., 2012. Permeability increase in Bowen Basin coal as a result of matrix shrinkage during primary depletion. Int. J. Coal Geol. 96-97, 109–119.
McCants, C., Spafford, S., Stevens, S., 2001. Five-Spot Production Pilot on Tight Spacing: Rapid Evaluation of a Coalbed Methane Block in the Upper Silesian Coal Basin, Poland.
Meng, Y., Li, Z., Lai, F., 2021. Influence of effective stress on gas slippage effect of different rank coals. Fuel 285, 119207.
Mukherjee, M., Bal, A., Misra, S., 2021. Role of Pore-size distribution in Coals to govern the Klinkenberg Coefficient and Intrinsic Permeability. Energy Fuel 35, 9561–9569.
Niu, Q., Wang, W., Liang, J., Yuan, W., Wen, L., Chang, J., Ji, Z., Zhou, H., Wang, Z., Jia, X., 2020. Investigation of the CO2 Flooding Behavior and its Collaborative Controlling Factors. Energy Fuel 34, 11194–11209.
Pan, Z., Connell, L.D., Camilleri, M., 2010. Laboratory characterisation of coal reservoir permeability for primary and enhanced coalbed methane recovery. Int. J. Coal Geol. 82, 252–261.
Ranathunga, A.S., Perera, M.S.A., Ranjith, P.G., Wei, C.H., 2017. An experimental investigation of applicability of CO2 enhanced coal bed methane recovery to low rank coal. Fuel 189, 391–399.
Sadasivam, S., Masum, S., Chen, M., Stańczyk, K., Thomas, H., 2022. Kinetics of gas phase CO2 adsorption on bituminous coal from a shallow coal seam. Energy Fuel 36, 8360–8370.
Sander, R., Connell, L.D., Pan, Z., Camilleri, M., Heryanto, D., Lupton, N., 2014. Core flooding experiments of CO2 enhanced coalbed methane recovery. Int. J. Coal Geol. 131, 113–125.
Seidle, J.P., Jeansonne, M.W., Erickson, D.J., 1992. Application of matchstick geometry to stress dependent permeability in coals. SPE Rocky Mountain Regional Meeting.
Shi, J.-Q., Mazumder, S., Wolf, K.-H., Durucan, S., 2008. Competitive methane desorption by supercritical CO2 injection in coal. Transp. Porous Media 75, 35–54.
Siriwardane, H., Haljasmaa, I., McLendon, R., Irdi, G., Soong, Y., Bromhal, G., 2009. Influence of carbon dioxide on coal permeability determined by pressure transient methods. Int. J. Coal Geol. 77, 109–118.
Stephen, A., Adebusuyi, A., Baldygin, A., Shuster, J., Southam, G., Budwill, K., Foght, J., Nobes, D.S., Mitra, S.K., 2014. Bioconversion of coal: new insights from a core flooding study. RSC Adv. 4, 22779–22791.
Viete, D.R., Ranjith, P.G., 2006. The effect of CO2 on the geomechanical and permeability behaviour of brown coal: Implications for coal seam CO2 sequestration. Int. J. Coal Geol. 66, 204–216.
Vishal, V., Ranjith, P.G., Pradhan, S.P., Singh, T.N., 2013. Permeability of sub-critical carbon dioxide in naturally fractured Indian bituminous coal at a range of down-hole stress conditions. Eng. Geol. 167, 148–156.
Wang, S., Elsworth, D., Liu, J., 2011. Permeability evolution in fractured coal: the roles of fracture geometry and water-content. Int. J. Coal Geol. 87, 13–25.
Wang, L., Chen, Z., Wang, C., Elsworth, D., Liu, W., 2019. Reassessment of coal permeability evolution using steady-state flow methods: The role of flow regime transition. Int. J. Coal Geol. 211.
Wei, M., Liu, J., Elsworth, D., Li, S., Zhou, F., 2019. Influence of gas adsorption induced non-uniform deformation on the evolution of coal permeability. Int. J. Rock Mech. Min. Sci. 114, 71–78.
Yin, G., Deng, B., Li, M., Zhang, D., Wang, W., Li, W., Shang, D., 2017. Impact of injection pressure on CO2–enhanced coalbed methane recovery considering mass transfer between coal fracture and matrix. Fuel 196, 288–297.
Zagorščak, R., Thomas, H.R., 2018. Effects of subcritical and supercritical CO2 sorption on deformation and failure of high-rank coals. Int. J. Coal Geol. 199, 113–123.
Zhang, X., Ranjith, P.G., 2019. Experimental investigation of effects of CO2 injection on enhanced methane recovery in coal seam reservoirs. J. CO2 Utiliz. 33, 394–404.
Zhou, F., Hussain, F., Cinar, Y., 2013. Injecting pure N2 and CO2 to coal for enhanced coalbed methane: Experimental observations and numerical simulation. Int. J. Coal Geol. 116-117, 53–62.